Generalized Exclusion Statistics in Astrophysics

Jaime Anguiano Olarra (jaimeangola.github@gmail.com)

April, 14th, 2023

Abstract

The free ideal gas of excitations following Polychronakos's fractional statistics is explored from a geometrical point of view. The introduction of a correction term used by other authors to the groundstate of pure bosons is also applied and compared to the bare case where this factor is not included. Later by a change of paradigm, the dependence of curvature on the fractional parameter is inverted into a relation for how the fractional parameter is affected by curvature,and the subsequent influence of this in the probability for a fractional parameter, the distribution of the number of particles and the internal energy is then evaluated for relevant cases as they travel through different curvatures in astrophysical conditions. A remarkable twist in the characterization of the level of fermionicity over curvature unveils under certain background conditions.

Introduction

The consequences of the statistics obeyed by field quanta is arguably one of the cornerstones of nature[1]. And yet its proof relies on unbroken symmetries in a world of broken symmetries. Fractional statistics, the umbrella covering the study of excitations which interpolate in between bosons and fermions, was originated in a time when there were no experimental reasons to explore the physics of those particles of the Third Kind (using Wilczek nomenclature[2]) but have proven useful and sometimes indispensable to explain experimental phenomena such as the Fractional Quantum Hall Effect[3].

Concomitantly, Information Geometry techniques to analyze spin-statistics has become a *go-to* tool, which might need not be regarded merely as a mathematical framework to characterize the distributions of many-body problems, and instead be embraced for a full fledged physical interpretation of its outcomes. A paradigmatic example where the crudity of the relation between geometry and information theory manifests is the Black Hole Information Paradox: the possible loss of information during black hole evaporation[4]. Here, and abstracting and generalizing, in other extended many-body systems whose components are subject, or suspected to be subject, to entanglement, that relation can turn literally physical, reminiscent of the classic figure where the event horizon is depicted as a binary grid [5]. It was in this arena that Bekenstein discovered the Area Law, which states that the entropy of black holes depends on their surface as we scale the source in contrast with the volume dependence. It was the first time this behavior common for entanglement entropies was found[6, 7, 22].

Fractional statistics quanta, which we will henceforth call anyons, can arise when one spatial dimension is inhibited, so in our world they are not expected in 3D[8]. This 2D world is the background in many experiments, e.g. the search of implementing quantum computing in such a promising status as to receive the attention and generous funding of the private sector[2, 9]. Now, this ruling out of an spatial dimension in astrophysical scenarios bring us back to the peculiar scenario previously pointed out, that of black holes. The equivalent of AdS_2[21] geometry in the vicinity of the horizon of an extreme Kerr black hole can be effectively considered two dimensional, hence, conditions for anyons to manifest there could be met[10]. Furthermore, this geometry (known as NHEK for Near Horizon Extreme Kerr)[11, 12], which can be taken as a proper space-time in its own right[21], exhibits a conformal symmetry along the throat of the hole that is an interesting sandbox for theoretical work. So the study of anyons might shed some light on this dark world which might host these excitations for which our standard 3D world seems hostile. The fact that observations so far suggest that supermassive black holes observed in the extremal regime are the rule rather than the exception encourage us to fully understand this geometry and the Physics therein. Towards that goal we take a first step.

The paper is organized as follows. In section 1 we review the basics of generalized exclusion statistics bringing in just the relevant *formulae* for our needs dressed in by a succinct presentation. In section 2 we summarize the essential elements of Information Geometry for later use. In section 3 we put all that to work in the case that concerns us, that of fractional statistics. In section 4 we take a complete different point of view and we study the behavior of a gas of anyons under the presence of gravity and we apply it to the specific background of a Kerr solution at realistic values of angular momentum. Finally the due discussion of the results brings the ending in section 5.

In the aim of providing an easy reproducibility of the results of this work, in the Appendix links are given to the Mathematica® notebooks containing results and formulae which extend the ones used here.

1. Quick review of generalized exclusion statistics

The idea behind fractional statistics, also called generalized exclusion statistics (GES), is answering a question that even the layperson thinks of when informed of the abrupt division between systems as they fall under the so-different Fermi-Dirac (FD) or Bose-Einstein (BE) statistics: is there anything else?. To this, Haldane[13] pioneered the concept of a new interpolating particle inspired by the quasiparticles in the Fractional Quantum Hall Effect [14]. Whereas his article was of utter importance we will be using our low brow version of an approach due to Polychronakos [15, 16]. Look back at the distribution function for the one particle states for the referred statistics at the limits: $\frac{1}{e^{\frac{\epsilon-\mu}{T}} \pm 1}$ (where the + sign is to be taken for fermions and the negative - for bosons) [17, 18]. In essence, the denominator differs in the sign of an additive constant of unitary value. The positive value disfavors the probability whereas the negative value is probability enhancing. We can naively replace it for a parameter, which we will be calling g, that takes on real values on the whole interval [-1, 1] and not only on its boundary. This is the pillar for our anyons. Particles obeying these statistics are said to be ruled by the general exclusion principle (which reduces to Pauli' s in the case of $g = 1$). We see that Boltzmann' s distribution, which applies in the classical limit, is obtained when g equals 0. It is worth warning that the different implementations of fractional statistics don't fully agree in all their results as for example happens with the third virial coefficient of the ideal anyon gas[8] which is radically different for statistics *a là* Polychronakos or *a là* Haldane.

The next stop in our summary comes from Wu's hand. In his seminal paper[19], he developed the statistical mechanics of these particles providing the Helmholtz potential as well as the Entropy, not only in general cases but also in the all important gas of free particles. Later, Nayak and Wilczek[14] elaborated on the previous works providing virial coefficients by resorting to the Sommerfeld expansion[14, 17, 20], and discovered an interesting duality: the exact behavior of anyons with parameter g and $\frac{1}{g}$. A modified version of this expansion was devised and used later by Aoyama[20] to compute the heat capacity of an anyon gas and, along the way, he found a closed form for the distribution function for values of g that are the inverse of a positive integer greater than one. The content of those papers will more than suffice for acquiring the knowledge requested in the following. The literature is enormous and we refer the reader to Khare's monography [8] for a broader and structured view. This accounts for our introduction to the subject.

Before we leave this section a comment on why we opt for the term anyon for this article is due. The term g-ons is widely used in literature and in deed it is more appropriate for the particles described here which come from Polychronakos' formulation, also named new fractional statistics. Even if there are sometimes subtle and sometimes greater differences in between the two, we use the term anyons because when coming into the realm of gravitation it may be confused with much older term for the quanta of geometrodynamics called geons, also, even pioneering authors in the field who referred to them as g-ons in the past[14], they finally embraced anyons[2].

2. Even quicker review of Information Geometry

Under a very appropriate name, in words of its founding father: "*Information geometry is a method of exploring the world of information by means of modern geometry*"[23]. The whole idea can also be stated as the answer to a question: can we visualize the difference in between two statistical distributions as a distance between them in some space?. The birth of a new branch of Mathematics arouse from there starting the incursion of Differential geometry machinery, and later on Topology, on the realm of statistics.

In particular by use of the Fisher-Rao metric[24], the differential geometry of the space of distribution functions is analyzed. From the works pioneered by Weinhold, and more influentially, by Ruppeiner, who used an entropy representation bridging the gap with Shannon's theory, Janyszek[25] arrived at the expression for metric of the parameter space in terms of the partition function[16, 26] which is nicely presented in many references[26] but here it is presented without proof.

$$g_{\mu\nu} = \frac{\partial^2 \text{Log}[Z]}{\partial \lambda^\mu \, \partial \lambda^\nu} \, (1)$$

Z is the partition function of the system and λ^μ and λ^ν are Lagrange multipliers of the Legendre transform of the entropy for the interested representation, and physically represent intensive variables constrained by the problem. We will be working with the grand canonical ensemble, that so, μ,ν take on two values, these intensive variables are $\lambda^1 = \beta = 1/T$ and $\lambda^2 = \gamma = -\mu/T$, being T the temperature of the system and in the last step, μ is not an index but the chemical potential. Implicitly Boltzmann's constant is disposed by sending it to one. Our manifold is then two dimensional. The scalar curvature can be computed from[26]:

$$R = 2 \; \frac{\begin{vmatrix} g_{\beta\beta} & g_{\gamma\gamma} & g_{\beta\gamma} \\ g_{\beta\beta,\beta} & g_{\gamma\gamma,\beta} & g_{\gamma\gamma,\beta} \\ g_{\beta\beta,\gamma} & g_{\gamma\gamma,\gamma} & g_{\gamma\gamma,\gamma} \end{vmatrix}}{\begin{vmatrix} g_{\beta\beta} & g_{\beta\gamma} \\ g_{\gamma\beta} & g_{\gamma\gamma} \end{vmatrix}^2} \; (2)$$

More conveniently, and henceforth, we will use the fugacity $z = e^{-\gamma}$ instead of γ.

Having geared up ourselves with the tools we needed from Information geometry we end this section. [24] makes a wonderful, although quite idiosyncratic detour on the subject.

3. The Geometry of Generalized Exclusion Statistics

Before embarking in computations, a warning. Our starting point will be the direct and comprehensive work by Mirza and Moham-madzadeh[16] who surveyed the presumably most relevant cases. For those who consult that paper please notice: in their article, when presenting the Polychronakos statistics, they use the same symbol "k" for two different entities. One of them is the Boltzmann constant, and the other a reparametrization of g. They introduce this change of variable from g to match the same limiting values of the fractional parameter (0 for bosons and 1 for fermions) with the one used by the other two statistics in their article, namely Gentile´s and Haldane´s.

In other to avoid confusion we rename their k to ρ. From here on, ρ will be our fractional parameter. Another problem arising from this reparametrization from g (α they use in [16]) in terms of ρ (their k in [16]) is that both the energy and the number of particles, as well as all the other magnitudes derived from them, they all become singular for $\rho = 1/2$ (the k in [16]). We circumvent this by evaluating on sufficiently adjacent values to it as to avoid these coordinate divergences. These close-to-but-not-1/2 values will be 0.499 and 0.501 unless a greater difference is needed (~0.489 or so sometimes is mandated to be able to plot results).

There is another combination of values that deserves some words. According to [16], the domain of the polylogarithm introduces a mathematical singular behavior when it is evaluated at z - 2ρz = 1, hence, for any fractional parameter ρ, there must be a divergence of the curvature at the critical value $z_c = 1/(1 - 2\rho)$. If we admit this argument, then we should really consider the inequality: z - 2ρz $\geq$ 1 as all those values would leak away of the function domain as we will show later. One last clarification, for brevity anyons, instead of an ideal gas of anyons will be frequently used.

We are now in a position to compute.

The internal energy of the system, the number of particles and the Helmholtz free energy are found to be in D dimensions:

$$U = \frac{A^D \beta^{-\frac{D}{\sigma}-1} \Gamma\left(\frac{D}{\sigma}+1\right) \mathrm{Li}_{\frac{D}{\sigma}+1}(z-2\rho z)}{(1-2\rho)\,\Gamma\left(\frac{D}{2}\right)} \; (3) \qquad N = \frac{A^D \beta^{-\frac{D}{\sigma}} \Gamma\left(\frac{D}{\sigma}\right) \mathrm{Li}_{\frac{D}{\sigma}}(z-2\rho z)}{(1-2\rho)\,\Gamma\left(\frac{D}{2}\right)} \; (4) \qquad F = -\frac{\sigma A^D \beta^{-\frac{D}{\sigma}} \Gamma\left(\frac{D+\sigma}{\sigma}\right) \mathrm{Li}_{\frac{D+\sigma}{\sigma}}(z-2z\rho)}{D\,(1-2\rho)\,\Gamma\left(\frac{D}{2}\right)} \; (5)$$

The expressions for the internal energy (3) and the number of particles (4) can be found in [16]. The expression for the free energy was obtained by integration from (3) with respect to β.

The parameter σ comes from the power of the energy of the single particle states in the dispersion relation which we assume to take the form: $\epsilon = A \cdot p^\sigma$[16, 26]. A is an overall constant that comes from the density of states for particles in a large box (or whatever other selected way for building the density of states function) which is: $G(\epsilon) = \frac{A^D}{\Gamma\left(\frac{D}{2}\right)} \epsilon^{\frac{D}{\sigma}-1}$. We also drop A in the numerical evaluations. The non-relativistic and ultrarelativistic cases are then given by σ values of 2 and 1 respectively.

It follows that we readily get the metric in the Polychronakos statistics by use of (3) and (4) in (1):

$$g_{\mu\nu} = \begin{pmatrix} g_{\beta\beta} & g_{\beta\gamma} \\ g_{\beta\gamma} & g_{\gamma\gamma} \end{pmatrix} = \begin{pmatrix} -\dfrac{A^D \beta^{-\frac{D}{\sigma}-2} \Gamma\left(\frac{D}{\sigma}+2\right) \mathrm{Li}_{\frac{D+\sigma}{\sigma}}(z-2z\rho)}{(2\rho-1)\,\Gamma\left(\frac{D}{2}\right)} & -\dfrac{A^D \beta^{-\frac{D+\sigma}{\sigma}} \Gamma\left(\frac{D+\sigma}{\sigma}\right) \mathrm{Li}_{\frac{D}{\sigma}}(z-2z\rho)}{(2\rho-1)\,\Gamma\left(\frac{D}{2}\right)} \\[2ex] -\dfrac{A^D \beta^{-\frac{D+\sigma}{\sigma}} \Gamma\left(\frac{D+\sigma}{\sigma}\right) \mathrm{Li}_{\frac{D}{\sigma}}(z-2z\rho)}{(2\rho-1)\,\Gamma\left(\frac{D}{2}\right)} & -\dfrac{A^D \beta^{-\frac{D}{\sigma}} \Gamma\left(\frac{D}{\sigma}\right) \mathrm{Li}_{\frac{D}{\sigma}-1}(z-2z\rho)}{(2\rho-1)\,\Gamma\left(\frac{D}{2}\right)} \end{pmatrix} \; (6)$$

The corresponding covariant derivative is: $D_\mu = g^{\mu\varepsilon}\left(-g_{\zeta\delta}\,\Gamma^\zeta_{\alpha\varepsilon} - g_{\alpha\zeta}\,\Gamma^\zeta_{\delta\varepsilon} + (\partial g)_{\varepsilon\alpha\delta}\right)$ (7)

and the scalar curvature matrix[26]:

$$
\begin{pmatrix} g_{\beta\beta} & g_{\gamma\gamma} & g_{\beta\gamma} \\ g_{\beta\beta,\beta} & g_{\gamma\gamma,\beta} & g_{\beta\gamma,\beta} \\ g_{\beta\beta,\gamma} & g_{\gamma\gamma,\gamma} & g_{\beta\gamma,\gamma} \end{pmatrix} = \begin{pmatrix} -\dfrac{A^{D}\beta^{-\frac{D}{\sigma}-2}\Gamma\left(\frac{D}{\sigma}+2\right)\mathrm{Li}_{\frac{D+\sigma}{\sigma}}(z-2z\rho)}{(2\rho-1)\Gamma\left(\frac{D}{2}\right)} & -\dfrac{A^{D}\beta^{-\frac{D}{\sigma}}\Gamma\left(\frac{D}{\sigma}\right)\mathrm{Li}_{\frac{D}{\sigma}-1}(z-2z\rho)}{(2\rho-1)\Gamma\left(\frac{D}{2}\right)} & -\dfrac{A^{D}\beta^{-\frac{D+\sigma}{\sigma}}\Gamma\left(\frac{D+\sigma}{\sigma}\right)\mathrm{Li}_{\frac{D}{\sigma}}(z-2z\rho)}{(2\rho-1)\Gamma\left(\frac{D}{2}\right)} \\[12pt] \dfrac{A^{D}\beta^{-\frac{D}{\sigma}-3}\Gamma\left(\frac{D}{\sigma}+3\right)\mathrm{Li}_{\frac{D+\sigma}{\sigma}}(z-2z\rho)}{(2\rho-1)\Gamma\left(\frac{D}{2}\right)} & \dfrac{A^{D}\beta^{-\frac{D+\sigma}{\sigma}}\Gamma\left(\frac{D+\sigma}{\sigma}\right)\mathrm{Li}_{\frac{D}{\sigma}-1}(z-2z\rho)}{(2\rho-1)\Gamma\left(\frac{D}{2}\right)} & \dfrac{A^{D}\beta^{-\frac{D}{\sigma}-2}\Gamma\left(\frac{D}{\sigma}+2\right)\mathrm{Li}_{\frac{D}{\sigma}}(z-2z\rho)}{(2\rho-1)\Gamma\left(\frac{D}{2}\right)} \\[12pt] \dfrac{A^{D}\beta^{-\frac{D}{\sigma}-2}\Gamma\left(\frac{D}{\sigma}+2\right)\mathrm{Li}_{\frac{D}{\sigma}}(z-2z\rho)}{(2\rho-1)\Gamma\left(\frac{D}{2}\right)} & \dfrac{A^{D}\beta^{-\frac{D}{\sigma}}\Gamma\left(\frac{D}{\sigma}\right)\mathrm{Li}_{\frac{D}{\sigma}-2}(z-2z\rho)}{(2\rho-1)\Gamma\left(\frac{D}{2}\right)} & \dfrac{A^{D}\beta^{-\frac{D+\sigma}{\sigma}}\Gamma\left(\frac{D+\sigma}{\sigma}\right)\mathrm{Li}_{\frac{D}{\sigma}-1}(z-2z\rho)}{(2\rho-1)\Gamma\left(\frac{D}{2}\right)} \end{pmatrix} \quad (8)
$$

The scalar curvature is then given by:

$$
R = -\frac{2(2\rho-1)\Gamma\left(\frac{D}{2}\right)\beta^{D/\sigma}\Gamma\left(\frac{D}{\sigma}+2\right)\Gamma\left(\frac{D}{\sigma}\right)\Gamma\left(\frac{D+\sigma}{\sigma}\right)\left(\mathrm{Li}_{\frac{D}{\sigma}-1}(z-2z\rho)\mathrm{Li}_{\frac{D}{\sigma}}(z-2z\rho)^{2}+\left(\mathrm{Li}_{\frac{D}{\sigma}-2}(z-2z\rho)\mathrm{Li}_{\frac{D}{\sigma}}(z-2z\rho)-2\mathrm{Li}_{\frac{D}{\sigma}-1}(z-2z\rho)^{2}\right)\mathrm{Li}_{\frac{D+\sigma}{\sigma}}(z-2z\rho)\right)}{\left(\Gamma\left(\frac{D+\sigma}{\sigma}\right)^{2}\mathrm{Li}_{\frac{D}{\sigma}}(z-2z\rho)^{2}-\Gamma\left(\frac{D}{\sigma}+2\right)\Gamma\left(\frac{D}{\sigma}\right)\mathrm{Li}_{\frac{D}{\sigma}-1}(z-2z\rho)\mathrm{Li}_{\frac{D+\sigma}{\sigma}}(z-2z\rho)\right)^{2}} \quad (9)
$$

These general results are now applied to different cases which are interesting to discuss and compared to the limits of Fermi-Dirac and Bose-Einstein distributions.

3.1 The 3D non-relativistic case:

The 3D case for the extremes of the fractional parameter, Bose-Einstein and Fermi-Dirac distributions, where reviewed recently[26], where for the case of bosons it was argued that much of the misunderstanding of the physical interpretation of the previous results by other authors[16], was due to the fact that the problem had been wrongly posed *ab initio*. Very reasonably they argued that the continuous approximation, assigning no particles to the groundstate, had to be corrected to properly describe the low temperature limit. As we are dealing with particles of a third kind, we can take advantage of this fact and freely track their steps in an unified view, not only on the boundary of the fractional parameter window, but in all its range both in what we call the bare case and after the Cafaro-Pessoa correction term is applied. Although the authors did not state explicitly the point[26], the correction to the groundstate cannot be applied to massless excitations like photons and phonons, so really it would apply not to all bosons, but only to massive ones, which otherwise is implicit in the use of the grand canonical partition function, meaning conserved number of particles, but if anyons could transient over different values of their character (adjusting individually or collectively their level of *fermionicity*), the number of particles could not be a sufficiently strong constrain and the system should be studied as a mixture. Besides, it would remain the problem of assigning the curvature to the groundstate. The correction chosen by Cafaro and Pessoa grants that it will be zero (flatness). It could be another constant value not necessarily zero and it could be that it has different local minima. Anyway we will see this problem would need to be attacked with a different correction term.

For ease of direct comparison with the results of Cafaro and Pessoa we will be closely following their steps.

3.1.1 From the bare metric

By setting the appropriate values in (6) the metric is found to be:

$$
g_{\mu\nu}^{[D3\sigma2]} = \begin{pmatrix} \dfrac{15\,\mathrm{Li}_{\frac{5}{2}}(z-2z\rho)}{\beta^{7/2}(4-8\rho)} & \dfrac{3\,\mathrm{Li}_{\frac{3}{2}}(z-2z\rho)}{\beta^{5/2}(2-4\rho)} \\[12pt] \dfrac{3\,\mathrm{Li}_{\frac{3}{2}}(z-2z\rho)}{\beta^{5/2}(2-4\rho)} & \dfrac{\mathrm{Li}_{\frac{1}{2}}(z-2z\rho)}{\beta^{3/2}(1-2\rho)} \end{pmatrix} \quad (10)
$$

Where we introduced the superscript $[Dd\sigma s]$ to indicate the dimension *d* and power of momentum *s*.

The scalar curvature matrix is:

$$
\begin{pmatrix} g_{\beta\beta} & g_{\gamma\gamma} & g_{\beta\gamma} \\ g_{\beta\beta,\beta} & g_{\gamma\gamma,\beta} & g_{\beta\gamma,\beta} \\ g_{\beta\beta,\gamma} & g_{\gamma\gamma,\gamma} & g_{\beta\gamma,\gamma} \end{pmatrix}^{[D3\sigma2]} = \begin{pmatrix} \dfrac{15\,\mathrm{Li}_{\frac{5}{2}}(z-2z\rho)}{\beta^{7/2}(4-8\rho)} & \dfrac{\mathrm{Li}_{\frac{1}{2}}(z-2z\rho)}{\beta^{3/2}(1-2\rho)} & \dfrac{3\,\mathrm{Li}_{\frac{3}{2}}(z-2z\rho)}{\beta^{5/2}(2-4\rho)} \\[12pt] -\dfrac{105\,\mathrm{Li}_{\frac{5}{2}}(z-2z\rho)}{2\beta^{9/2}(4-8\rho)} & -\dfrac{3\,\mathrm{Li}_{\frac{1}{2}}(z-2z\rho)}{2\beta^{5/2}(1-2\rho)} & -\dfrac{15\,\mathrm{Li}_{\frac{3}{2}}(z-2z\rho)}{2\beta^{7/2}(2-4\rho)} \\[12pt] \dfrac{15\,(2\rho z-z)\mathrm{Li}_{\frac{3}{2}}(z-2z\rho)}{\beta^{7/2}(4-8\rho)(z-2\rho z)} & \dfrac{(2\rho z-z)\mathrm{Li}_{-\frac{1}{2}}(z-2z\rho)}{\beta^{3/2}(1-2\rho)(z-2\rho z)} & \dfrac{3\,(2\rho z-z)\mathrm{Li}_{\frac{1}{2}}(z-2z\rho)}{\beta^{5/2}(2-4\rho)(z-2\rho z)} \end{pmatrix} \quad (11)
$$

Leading us to the scalar curvature:

$$R = -\frac{20\,\beta^{3/2}\,(2\,\rho-1)\left(\mathrm{Li}_{\frac{1}{2}}(z-2\,z\,\rho)\,\mathrm{Li}_{\frac{3}{2}}(z-2\,z\,\rho)^2+\left(\mathrm{Li}_{-\frac{1}{2}}(z-2\,z\,\rho)\,\mathrm{Li}_{\frac{3}{2}}(z-2\,z\,\rho)-2\,\mathrm{Li}_{\frac{1}{2}}(z-2\,z\,\rho)^2\right)\mathrm{Li}_{\frac{5}{2}}(z-2\,z\,\rho)\right)}{\left(3\,\mathrm{Li}_{\frac{3}{2}}(z-2\,z\,\rho)^2-5\,\mathrm{Li}_{\frac{1}{2}}(z-2\,z\,\rho)\,\mathrm{Li}_{\frac{5}{2}}(z-2\,z\,\rho)\right)^2} \quad (12)$$

The metric determinant appears as the denominator in the Ricci scalar so it is not a bad idea to check its behavior. If we not restrict ourselves to the values for the fugacity explored recently[26] as justified above, we obtain for different values of the fractional parameter:
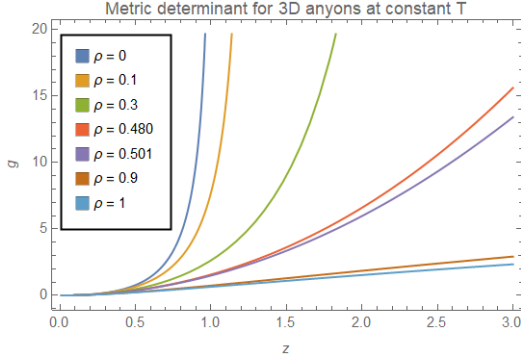
Figure 1. The determinant of the metric as a function of fugacity for a set of different fractional parameter values.

Computing the curvature through (12) we obtain modest positive values for the bosonic sector ($0 < \rho < 0.5$) and observe their decay towards flatness as the fractional parameter approaches 1/2, a frontier that once crossed, curvature turns negative, but also almost flat, to keep dimly, increasing in absolute value while maintaining its negative character in the fermionic sector ($0.5 < \rho < 1$). The dependence on fugacity in this range seems weak. Regarding temperature, the bosonic sector increases its curvature with it and the fermionic sector drifts into values more and more negative with it, exposing a somewhat symmetric behavior but of opposite sign.
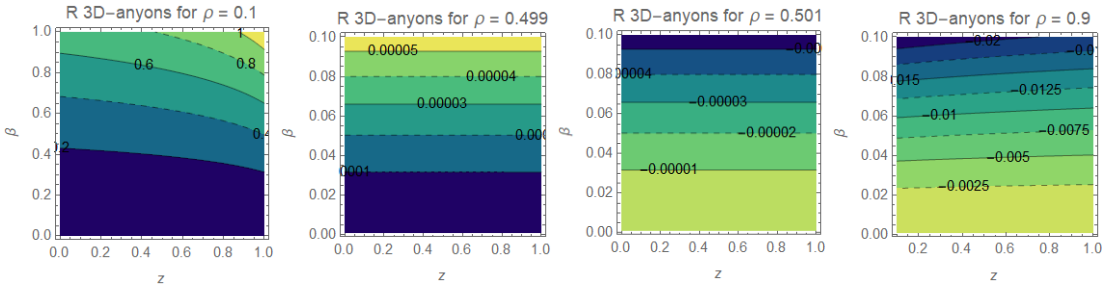
Figure 2. Contour plots of curvature for a set of fractional parameter values ranging from the close bosonic sector ($\rho \sim 0$) reaching to the close fermionic sector ($\rho \sim 1$) .

Consistently we arrive at the same results when line plots are used as was done in [26] for bosons. There is no new information in Figure 3. but the different representation eases the reading. Reducing the temperature reduces the curvature and for low fugacities the absolute value of curvature is almost fugacity independent for all values of the statistical parameter being almost flat for borderline anyons $\rho \sim 1/2$ (classical limit).
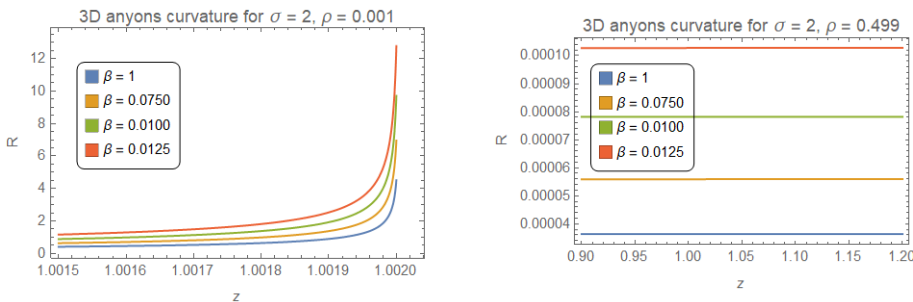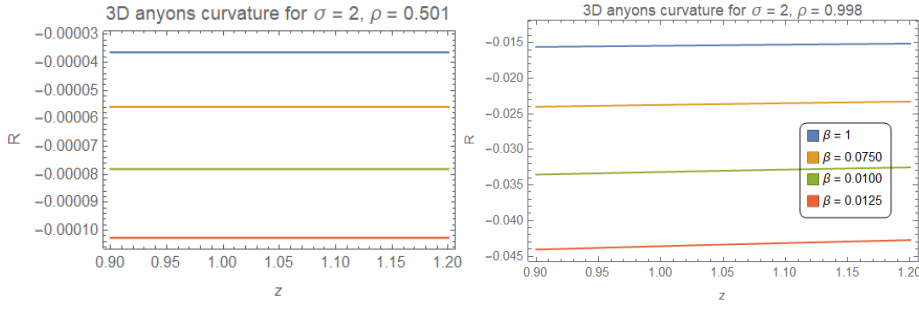
Figure 3. Curvature for a set of fractional parameter values ranging from the close bosonic sector ($\rho \sim 0$) reaching to the close fermionic sector ($\rho \sim 1$) .

When we turn our attention to the curvature as a function of the fractional parameter of given value of z for which we observe a dull behavior and a smooth transition at the $\rho = 1/2$ point:
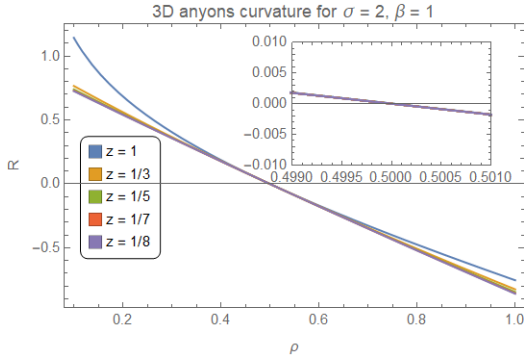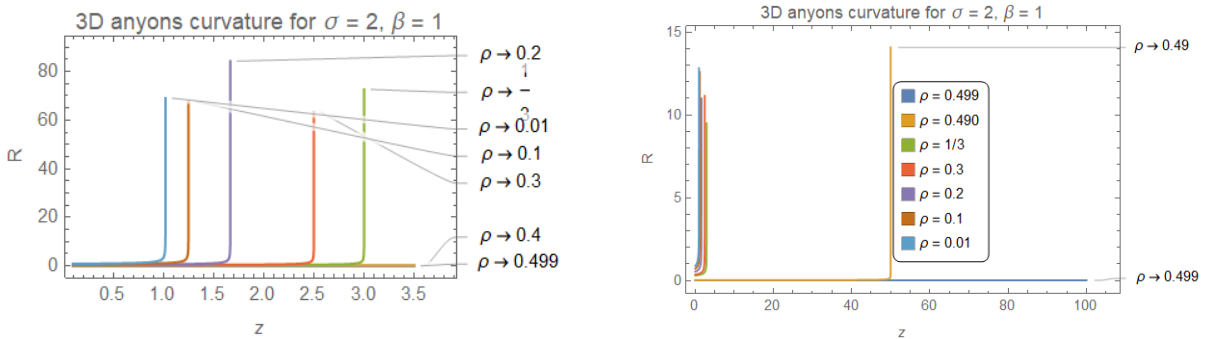

Figure 4. Curvature in terms of the fractional parameter for a different values in the low limit of fugacity.

This is not all to the problem. There is a so much richer structure in our case than in the limited BE/FD statistics. As mentioned above, Mirza and Mohammadzadeh[16] noticed that for any given value of ρ differing from unity, the curvature would be singular at a certain critical value of the fugacity. Figures 5 and 6 show a skyrocketing curvature as predicted by they, it doesn't fully blow up in the plots although neither it comes back to lower values, it simply rises up to a certain level just to vanish then onward, coinciding with our interpretation that the critical fugacity should not be seen as a point singularity but as an horizon. Another feature that we can infer from the these plots is that there seems to be an alternating pattern in the maxima of the curvature for adjacent values of the fractional parameter suggesting that even if the real behavior (analytically) is asymptotic to infinite curvature, the rates at which this achieved might be different, something we won't dwell into in the present work. Nevertheless from this results, we agree with [16], at these values of fugacity and fractional parameter where the curvature blows up condensation takes place and the correction to the groundstate that effectively works for FD and BE, cannot avoid this in our case.

Figures 5 and 6. Curvature as a function of fugacity for different values of the fractional parameter in the bosonic sector. We observe the behavior of BE-condensation-like first described in [16].

The fermionic sector shows no divergence and as we leave the classical limit ($\rho \sim 0.5$) and we cruise to the pure fermionic limit.
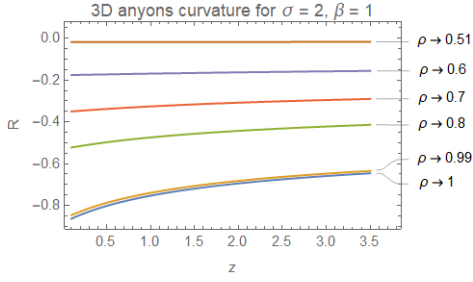
Figure 7. Curvature as a function of fugacity for different values of the fractional parameter in the fermionic sector.

As depicted in Figure 7, by contrast, in the fermionic sector there are no divergences. The borderline cases are almost flat, and so they keep all the way up to very high levels of fermionicity. 3D plots in the (z, ρ, R) space are shown in Figure 8. The singular behavior of R can be easily perceived. Remember that this is really a continuous barrier and that unless ρ or z should be of discrete nature, the appearance of these spikes are an artifact due to the sampling in the construction of the plots.
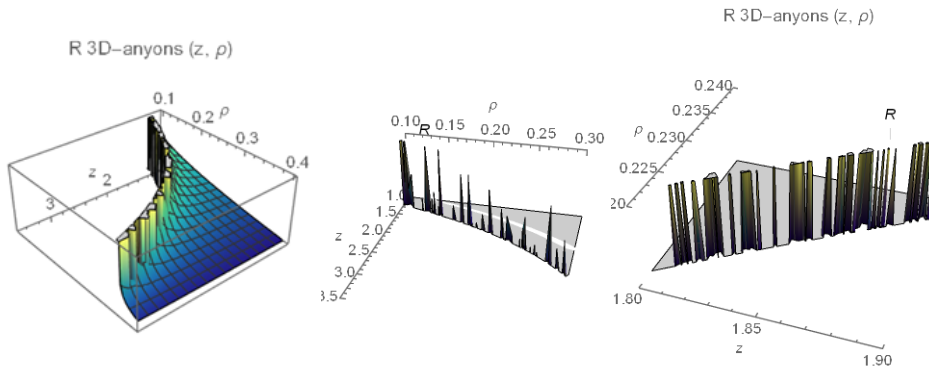
Figure 8. 3D plots in the (z, ρ, R) space show the rim exhibited when the condition predicted[16] is met. Sampling different ranges of the fractional parameter explicitly show that the structure is really that of a continuous cut as long as ρ and z take on continuous values.

As we travel closer to the fermionic sector, but while remaining in the bosonic sector, higher fugacities are needed for this leaps of curvature to happen. In the fermionic sector, as already pointed out[16] none of this type of singularities arise. There is no BE-condensation-like in the fermionic sector. What would happen if we consider the correction to the groundstate?.

3.1.2 Under the Cafaro-Pessoa correction to the groundstate

The correction introduced by Cafaro and Pessoa[26] is: $N_0 = \frac{1}{z^{-1}-1}$, an additive term to the number of particles (4). This correction term affects the metric in the entry for the double differentiation of the partition function with respect to γ, the wrap of the chemical potential, which we dressed up with an exponential map to another function, fugacity, in the previous subsection. The metric thence turns into:

$$g_{\mu\nu}^{[D3\sigma2]} = \begin{pmatrix} \frac{15\,\mathrm{Li}_{\frac{5}{2}}(z-2\,z\,\rho)}{\beta^{7/2}\,(4-8\,\rho)} & \frac{3\,\mathrm{Li}_{\frac{3}{2}}(z-2\,z\,\rho)}{\beta^{5/2}\,(2-4\,\rho)} \\ \frac{3\,\mathrm{Li}_{\frac{3}{2}}(z-2\,z\,\rho)}{\beta^{5/2}\,(2-4\,\rho)} & \frac{\mathrm{Li}_{\frac{1}{2}}(z-2\,z\,\rho)}{\beta^{3/2}\,(1-2\,\rho)} + \frac{z}{(z-1)^2} \end{pmatrix} \quad (14)$$

Where we coloured the modification for the reader convenience.

It then follows that the scalar curvature matrix now has two entries modified:

$$\begin{pmatrix} g_{\beta\beta} & g_{\gamma\gamma} & g_{\beta\gamma} \\ g_{\beta\beta,\beta} & g_{\gamma\gamma,\beta} & g_{\beta\gamma,\beta} \\ g_{\beta\beta,\gamma} & g_{\gamma\gamma,\gamma} & g_{\beta\gamma,\gamma} \end{pmatrix}^{[D3\sigma2]} = \begin{pmatrix} \frac{15\,\mathrm{Li}_{\frac{5}{2}}(z-2\,z\,\rho)}{\beta^{7/2}\,(4-8\,\rho)} & \frac{\mathrm{Li}_{\frac{1}{2}}(z-2\,z\,\rho)}{\beta^{3/2}\,(1-2\,\rho)} + \frac{z}{(z-1)^2} & \frac{3\,\mathrm{Li}_{\frac{3}{2}}(z-2\,z\,\rho)}{\beta^{5/2}\,(2-4\,\rho)} \\ -\frac{105\,\mathrm{Li}_{\frac{5}{2}}(z-2\,z\,\rho)}{2\,\beta^{9/2}\,(4-8\,\rho)} & -\frac{3\,\mathrm{Li}_{\frac{1}{2}}(z-2\,z\,\rho)}{2\,\beta^{5/2}\,(1-2\,\rho)} & -\frac{15\,\mathrm{Li}_{\frac{3}{2}}(z-2\,z\,\rho)}{2\,\beta^{7/2}\,(2-4\,\rho)} \\ \frac{15\,(2\,\rho\,z-z)\,\mathrm{Li}_{\frac{3}{2}}(z-2\,z\,\rho)}{\beta^{7/2}\,(4-8\,\rho)\,(z-2\,\rho\,z)} & \frac{(2\,\rho\,z-z)\,\mathrm{Li}_{-\frac{1}{2}}(z-2\,z\,\rho)}{\beta^{3/2}\,(1-2\,\rho)\,(z-2\,\rho\,z)} + \frac{2}{(z-1)^3\,z^2} - \frac{z}{(z-1)^2} & \frac{3\,(2\,\rho\,z-z)\,\mathrm{Li}_{\frac{1}{2}}(z-2\,z\,\rho)}{\beta^{5/2}\,(2-4\,\rho)\,(z-2\,\rho\,z)} \end{pmatrix} \quad (15)$$

Leading us to the scalar curvature:

$$R = -\frac{90\,\beta^{3/2}\,(1-2\,\rho)^4\,(z-1)^4\,R_1}{(2\,\rho-2\,\rho\,z+z-1)^3\,R_2{}^2} \quad (16)$$

Where we introduced the expressions R_1 and R_2 for editing purposes.

$$R_1 = 2\,\mathrm{Li}_{\frac{5}{2}}(z - 2\,z\,\rho)\,\mathrm{Li}_{\frac{3}{2}}(z - 2\,z\,\rho)\left(\frac{\beta^{3/2}\,(2\,\rho-1)\,((z-1)\,z^3-2)}{z^2} - (z - 1)^3\,\mathrm{Li}_{-\frac{1}{2}}(z - 2\,z\,\rho)\right)$$

$$+(1 - z)\,\mathrm{Li}_{\frac{3}{2}}(z - 2\,z\,\rho)^2\left(2\,(z - 1)^2\,\mathrm{Li}_{\frac{1}{2}}(z - 2\,z\,\rho) + 5\,\beta^{3/2}\,(1 - 2\,\rho)\,z\right)$$

$$-(1 - z)\,\mathrm{Li}_{\frac{1}{2}}(z - 2\,z\,\rho)\,\mathrm{Li}_{\frac{5}{2}}(z - 2\,z\,\rho)\left(4\,(z - 1)^2\,\mathrm{Li}_{\frac{1}{2}}(z - 2\,z\,\rho) + 7\,\beta^{3/2}\,(1 - 2\,\rho)\,z\right)$$

$$R_2 = 9\,(z - 1)^2\,\mathrm{Li}_{\frac{3}{2}}(z - 2\,z\,\rho)^2 - 15\,\mathrm{Li}_{\frac{5}{2}}(z - 2\,z\,\rho)\left((z - 1)^2\,\mathrm{Li}_{\frac{1}{2}}(z - 2\,z\,\rho) + \beta^{3/2}\,(1 - 2\,\rho)\,z\right)$$

Repeating what we did in the previous subsection the results are now:
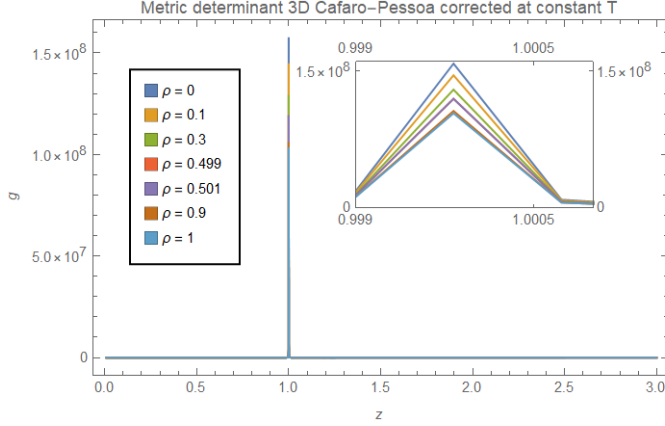
Figure 9. The determinant of the metric as a function of fugacity for a set of different fractional parameter values after correction.

As easy to read from the correction parameter itself and as shown in the figure, it makes the metric of the determinant diverge at the unitary value of the fugacity. As this factor appears in the denominator of the curvature, it effectively cancels the otherwise unbounded curvature at that only value of the fugacity. But, in the case of the particles of the third kind, as it doesn't affect any other value of z it cannot cope with curvature diverging at the matching condition for ρ and z. For that to happen, if we wanted to impose this non-divergency condition, a correction term depending of both z and ρ would be needed, as the astute reader surely anticipated. And it would need to be so that it could compensate the divergence coming along the curve z = 1/(1-2ρ). This is too much fine tuning to look correct in our opinion.

When we run the same experiments with the new metric we arrive at completely different results from those of the previous section, curvature becomes extremely fugacity dependant, always divergent as fugacity decreases for the bosonic sector, and only bounded in the case of fermionic anyons if fugacity is high enough and never less than 1 (Fig. 10).
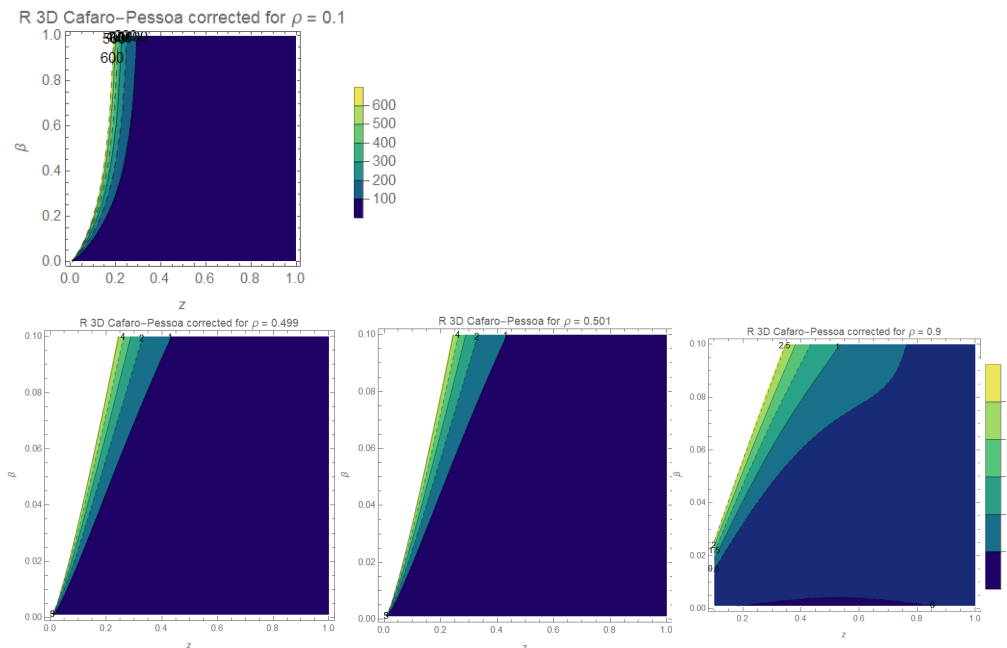
Figure 10. Contour plots of curvature for a set of fractional parameter values ranging from the close bosonic sector ($\rho \sim 0$) reaching to the close fermionic sector ($\rho \sim 1$) after correction.
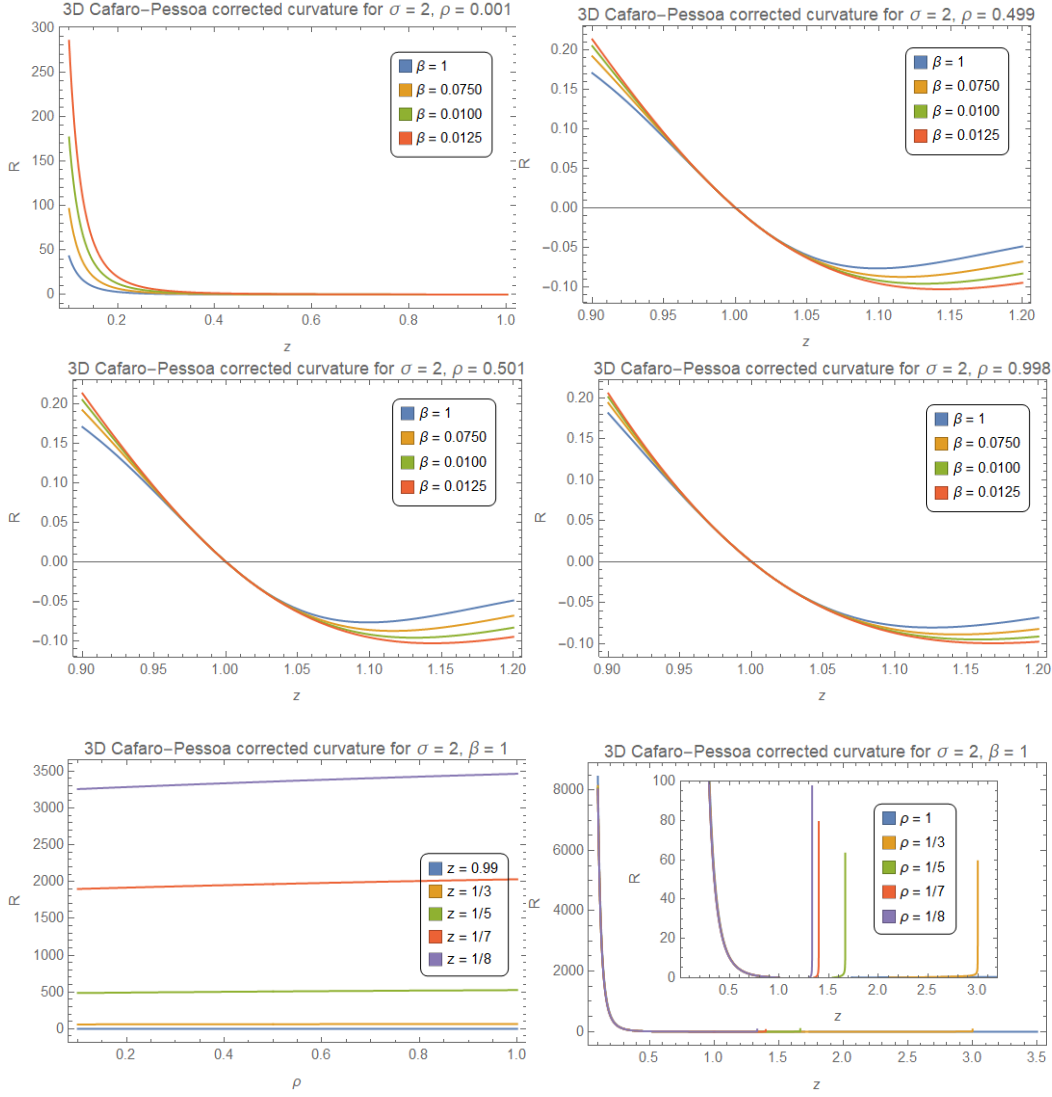

Figure 11. Curvature as a function of fugacity for different values of the fractional parameter in the bosonic sector. Bose-Einstein-like condensation, first described in [16], persists after correction.

The added term does change the situation notably in the fermionic sector where it wasn't needed in first place. It in deed tamed the pure bosons' curvature, but it is not enough for the rest of the fractional statistics particles that belong to the bosonic sector.

3.2 The ultrarelativistic case

The case $\sigma = 1$ gives results very similar to the ones of the non-relativistic case. Having analyzed the galilean case in detail. We will only comment briefly the present one.

As the correction term proved useless to our interests, we leave it out in the forthcoming.

Metric, scalar curvature matrix and scalar curvature take the respective forms:

$$g_{\mu\nu}^{[D3\sigma1]} = \begin{pmatrix} \frac{48\,\mathrm{Li}_4(z-2\,z\,\rho)}{\sqrt{\pi}\,\beta^5\,(1-2\,\rho)} & \frac{12\,\mathrm{Li}_3(z-2\,z\,\rho)}{\sqrt{\pi}\,(\beta^4-2\,\beta^4\,\rho)} \\ \frac{12\,\mathrm{Li}_3(z-2\,z\,\rho)}{\sqrt{\pi}\,(\beta^4-2\,\beta^4\,\rho)} & \frac{4\,\mathrm{Li}_2(z-2\,z\,\rho)}{\sqrt{\pi}\,(\beta^3-2\,\beta^3\,\rho)} \end{pmatrix} \quad (17)$$

$$
\begin{pmatrix} g_{\beta\beta} & g_{\gamma\gamma} & g_{\beta\gamma} \\ g_{\beta\beta,\beta} & g_{\gamma\gamma,\beta} & g_{\beta\gamma,\beta} \\ g_{\beta\beta,\gamma} & g_{\gamma\gamma,\gamma} & g_{\beta\gamma,\gamma} \end{pmatrix}^{[D3\sigma1]} = \begin{pmatrix} \dfrac{48\,\mathrm{Li}_4(z-2\,z\,\rho)}{\sqrt{\pi}\,\beta^5\,(1-2\,\rho)} & \dfrac{4\,\mathrm{Li}_2(z-2\,z\,\rho)}{\sqrt{\pi}\,(\beta^3-2\,\beta^3\,\rho)} & \dfrac{12\,\mathrm{Li}_3(z-2\,z\,\rho)}{\sqrt{\pi}\,(\beta^4-2\,\beta^4\,\rho)} \\[2mm] -\dfrac{240\,\mathrm{Li}_4(z-2\,z\,\rho)}{\sqrt{\pi}\,\beta^6\,(1-2\,\rho)} & -\dfrac{4\,(3\,\beta^2-6\,\beta^2\,\rho)\,\mathrm{Li}_2(z-2\,z\,\rho)}{\sqrt{\pi}\,(\beta^3-2\,\beta^3\,\rho)^2} & -\dfrac{12\,(4\,\beta^3-8\,\beta^3\,\rho)\,\mathrm{Li}_3(z-2\,z\,\rho)}{\sqrt{\pi}\,(\beta^4-2\,\beta^4\,\rho)^2} \\[2mm] \dfrac{48\,(2\,\rho\,z-z)\,\mathrm{Li}_3(z-2\,z\,\rho)}{\sqrt{\pi}\,\beta^5\,(1-2\,\rho)\,(z-2\,\rho\,z)} & -\dfrac{4\,(2\,\rho\,z-z)\,\log(2\,\rho\,z-z+1)}{\sqrt{\pi}\,(\beta^3-2\,\beta^3\,\rho)\,(z-2\,\rho\,z)} & \dfrac{12\,(2\,\rho\,z-z)\,\mathrm{Li}_2(z-2\,z\,\rho)}{\sqrt{\pi}\,(\beta^4-2\,\beta^4\,\rho)\,(z-2\,\rho\,z)} \end{pmatrix} \quad (18)
$$

$$
R = \frac{2\,\sqrt{\pi}\,\beta^3\,(2\,\rho-1)\,(\mathrm{Li}_4(z-2\,z\,\rho)\,(2\,\mathrm{Li}_2(z-2\,z\,\rho)^2+\mathrm{Li}_3(z-2\,z\,\rho)\,\log(2\,\rho\,z-z+1))-\mathrm{Li}_2(z-2\,z\,\rho)\,\mathrm{Li}_3(z-2\,z\,\rho)^2)}{(3\,\mathrm{Li}_3(z-2\,z\,\rho)^2-4\,\mathrm{Li}_2(z-2\,z\,\rho)\,\mathrm{Li}_4(z-2\,z\,\rho))^2} \quad (19)
$$

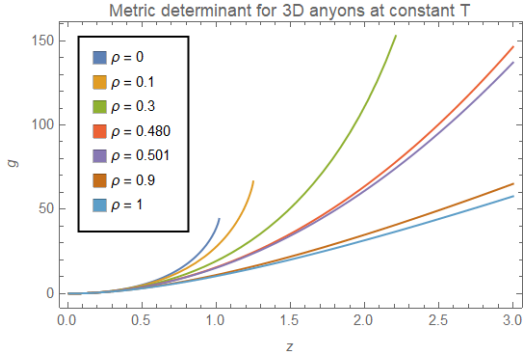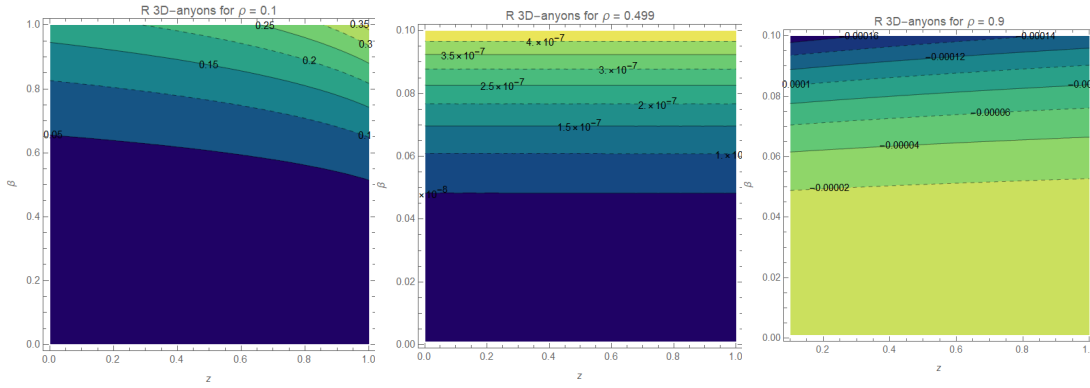

Figure 12. The determinant of the metric as a function of fugacity for a set of different fractional parameter values (ultrarelativistic)
The determinant of the metric languishes compare to its non-relativistic bare counterpart, nevertheless to diverge.

Figure 13. Contour plots of curvature for a set of fractional parameter values ranging from the highly bosonic sector ($\rho \sim 0$) reaching to the highly fermionic sector ($\rho \sim 1$) (ultrarelativistic).

The curvatures have match qualitative the behavior of their galilean counterparts but the absolute values of their magnitude is smaller (c.ref. Fig. 4).
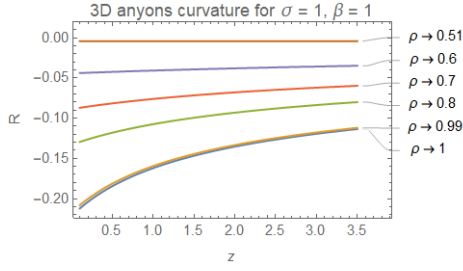
Figure 14. Curvature as a function of fugacity for different values of the fractional parameter in the bosonic sector (first caption), as a function of the fractional parameter for different values of the fugacity (middle caption) and in the fermionic sector (last caption). We observe the behavior of Bose-Einstein condensation first described in [16] also manifests in the ultrarelativistic limit.

It follows that the ultrarelativistic case barely differs from the non-relativistic one. This could be anticipated by inspection realizing that, although the metric changed from the non-relativistic case, the essential feature of the condition for the parameters of the polylogarithm did not. Because of this very reason, the correction here, if applied, would yield results not much different.

This marks the end of our study of the Information geometry of anyons.

4. The behavior of the anyon gas in astrophysical conditions

4.1 Fractional parameter as a function of curvature and temperature

Now we turn the previous problem upside down. The point of view to take is very much like in the analogy posed by one of Robertson's students, that of a person taking measurements with a ruler on a hot plate[27]. There, the temperature field would look to a experimenter who considers it to be homogeneous and isotropic that is her ruler that changes as it moves between hither and yon, not realizing that it is the environment what makes the change in the ruler. Our hot plate is the space where the gas of anyons lives. The anyons feel now the curvature and temperature of the space that hosts them and the assumption here is that they respond in the same way as they expressed curvature. As they are a lump in free motion in empty space, the fugacity is going to be considered small in this first survey.

We use the ultrarelativistic case of 3D anyons, which might fit better for quanta travelling in the target space of the vicinity of the singularity of an extreme Kerr black hole. We could have equally well used the galilean case if we consider an asymptotically flat region of interstellar media.

We are going to need $\rho = \rho(\beta, z, R)$. Deriving it from the expression for R, if given by (19) we are doomed. It would make no sense at this point to look for precision at the cost of clarity and computability so we come to the compromise of transforming R by taking as many first order series as necessary of the polylogarithm functions it contains.

The result remains daunting:

$$R = \frac{1}{(3\,\mathrm{Li}_3(z)^2 - 4\,\mathrm{Li}_2(z)\,\mathrm{Li}_4(z))^3}\,2\,\sqrt{\pi}\,\beta^3\left(\mathrm{Li}_3(z)^3\left(-4\,\rho\,\mathrm{Li}_2(z)^2 + 3\,(1-2\,\rho)\,\mathrm{Li}_3(z)\,\mathrm{Li}_2(z) + 12\,\rho\,\mathrm{Li}_3(z)\,(\mathrm{Li}_3(z) + \log(1-z))\right) + \quad (21)$$
$$4\,\mathrm{Li}_4(z)^2\left((2-4\,\rho)\,\mathrm{Li}_2(z)^3 - 4\,\rho\,\mathrm{Li}_3(z)\,\log^2(1-z) - 2\,\rho\,\mathrm{Li}_2(z)^2\,\log(1-z) + \mathrm{Li}_3(z)\,\mathrm{Li}_2(z)\left(\log(1-z) - \right.\right.$$
$$\left.\left. 4\,\rho\,\tanh^{-1}(1-2\,z)\right)\right) - \mathrm{Li}_4(z)\,\mathrm{Li}_3(z)^2\left((10-20\,\rho)\,\mathrm{Li}_2(z)^2 + 2\,\rho\,\mathrm{Li}_2(z)\,(8\,\mathrm{Li}_3(z) + \right.$$
$$\left.\left. 13\,\log(1-z)) + 3\,\mathrm{Li}_3(z)\left(\log(1-z) - 4\,\rho\,\tanh^{-1}(1-2\,z)\right)\right)\right)$$

Nevertheless it allows for a numerical evaluation and this suffices for our purposes at this stage.
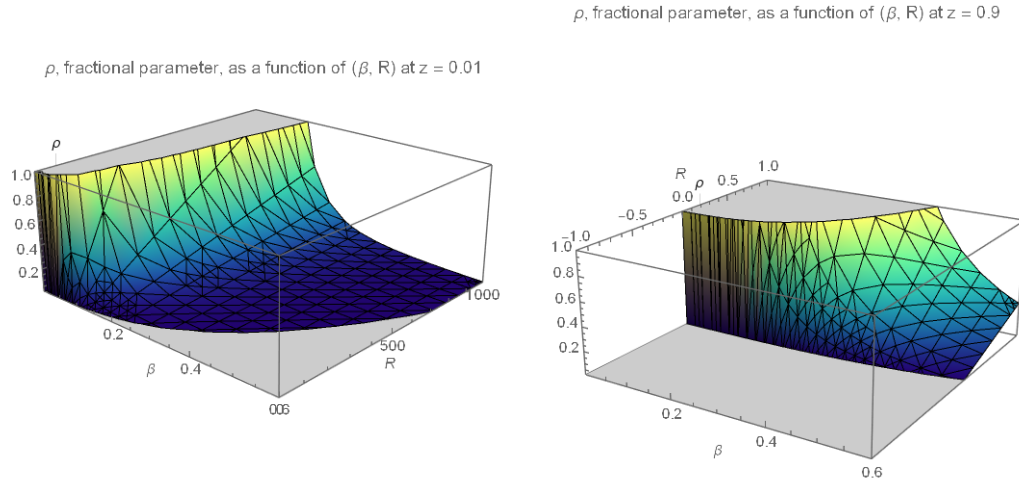
Fig. 15. Fractional parameter as a function of low β and R for fugacity values z = 0.01 and z = 0.9 respectively (3D ultrarelativistic) derived from (21).

According to Figure 15 non very bosonic anyons can live only in a certain range of temperature for a given a curvature that they might be exposed to, at least as long as their fugacity is kept very low (z = 0.01 was used). We also see that the bosonic sector is slightly favoured and curvature enhances this asymmetry. At a given fugacity or for β high, which dominates over z in most of the domain, from Fig. 15, an approximate fit can be constructed by inspection and some trial and error. For up to moderate values of curvature we can write:

$$\rho\,(\beta,\ R)\ =\ e^{-(\beta^{1/\beta}+\beta)}\,\log(R)\left(1\,-\,e^{-(\beta+\log(R))^2}\right)\ (22)$$

But we are not done, for Fig. 15 is also saying that the fractional parameter doesn't exist for negative values of R. This contradicts what we have already witnessed all this way, these values for ρ correspond to the fermionic sector. This signals a problem with (21) and (22).

After working many different alternative expressions for $\rho\,(\beta, R)$ in terms of numerically solving for ρ (for instance taking series up to four terms of the polylogarithms recursively until only logarithms are left and/or adding the substitution of series of the logarithms, polylogarithms at different stages, and a full fledge substitution of whatnot till arriving at a expressions for R like (23)) nothing ended up working in a reliable way. *Exempli gratia*, one such transforms tried, was:

$$R = \frac{2\ \sqrt{\pi}\ \beta^3\,(2\,\rho-1)\left(-\frac{1}{3}\times 2\,\rho\,z^2\left(\frac{2\,\rho\,(z(z(4\,\rho^2+6\,\rho-(\rho\,(6\,\rho^2+4\,\rho+3)+3)\,z+9)-3\,(\rho+3))+3)}{(z-1)^4}-3\right)+(z-2\,\rho\,z)^2+z\right)}{(z-2\,\rho\,z)^3}\ (23)$$

Neither (21) nor (23) gives the right ρ when run against the cases studied in the previous section as a check. The results obtained by these won't be fully discarded, but they need to be taken cautiously accepting their fragility. Considering that we are interested in applying this to the specific case described in a later subsection, which requires low z, high β and up to very large absolute values of curvature, we obtained an "empirical" expression based on the results of the previous subsection:

$$\rho\,(\beta, R) = \frac{2.324481683262958\times 10^8 - R}{(4.648963366525916\times 10^8)\,\beta^3}\quad (24)$$

Withal, the physical consequence of (24) and whatever other expression used, is that subject to a gravitational and/or temperature field, there is a natural selection of fractional parameter. In a theory of an anyonic ideal gas whose constituent particles can adjust its fractional parameter, those would transient themselves to acquire the proper values, at least collectively, while for models which keep the fractional parameter fixed, these plots represent how the different particles or clusters of them with a certain coarse-grained parameter would distribute.

If no risk is wanted to be assumed, nothing in the rest of this subsection is needed for the next and last one, which deals solely with results obtained by use of (24) and could be, therefore, trusted. The main disadvantage in skipping the rest of the present one is that the interpretation of the results will be restricted to that applied case where no other value of fugacity different from 0.1 will be considered.

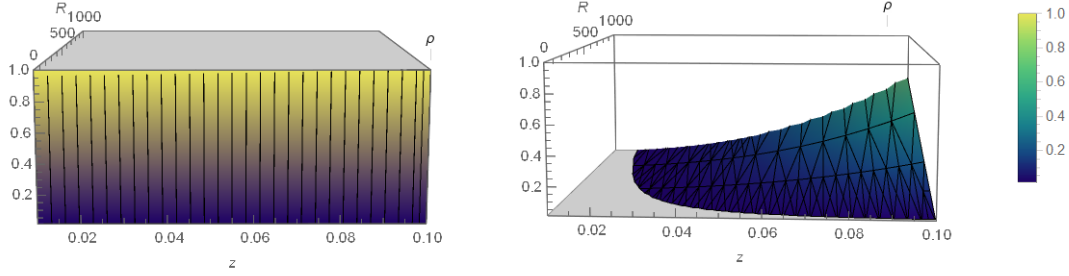With this in mind we proceed with our analysis.

Fig. 16. Fractional parameter as a function of fugacity (in its lower limit) and curvature for $\beta = 0.003$ and for $\beta = 1$ respectively (3D ultrarelativistic) using numerical evaluation for obtaining ρ by use of (21). But (21) is flawed so this results might only be qualitative (see main text).

If terms of fugacity dependance, in the low limit, giving some validity to Fig. 16, it shows that at very low β we have a reminiscence of a "fermi surface" filled with mostly highly fermionic anyons and a portion of highly bosonic excitations but no intermediate fractional values, in contrast with the behavior as temperature drops, getting almost no particles from highly fermionic sector at any curvature when β is unitary (right of the figure). As fugacity increases, the excitations behave more like fermions (or only very fermionic particles are allowed, as we said). This is depicted in Figure 17.

Unavoidably, according to (21), at $z = 1$, another side of the "fermi surface" appears and no fractional excitations live beyond.
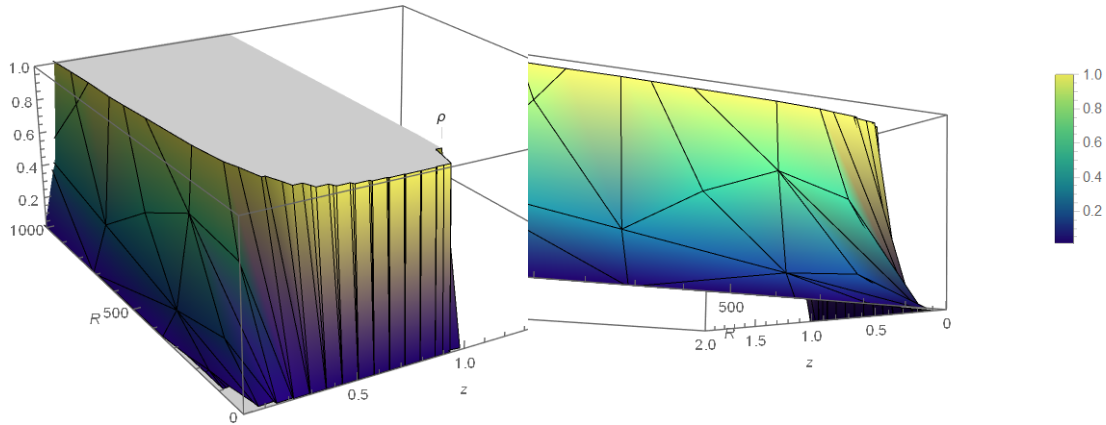
Fig. 17. Fractional parameter as a function of fugacity (in its lower limit) and curvature for $\beta = 1$ (3D ultrarelativistic). These were obtained by numerical reversing (21) so results could only be qualitatively considered in the best of cases.
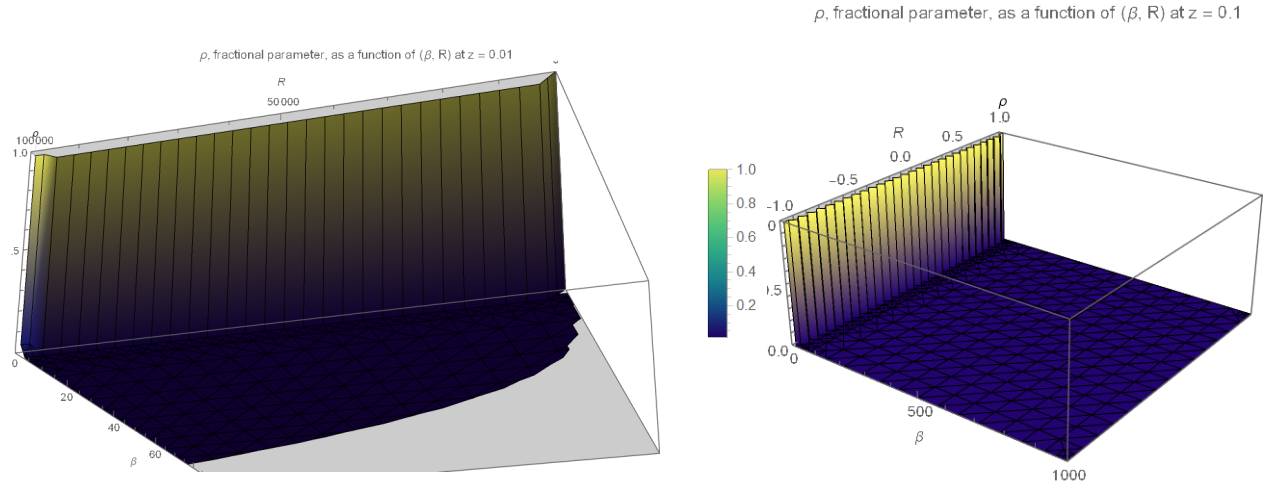
Fig. 18. Fractional parameter as a function of β (in long range) and curvature (3D ultrarelativistic). Left.: obtained by numerical reversing (21) and with z = 0.01. Right: obtained by using (24), and thence, for z = 0.1. Although the two plots look very similar, a detailed inspection of the scope of R shows that the results are very different as those coming from (21) are null from flatness to negative values. Nevertheless the concordant picture for positive values of R brings some relief to the dodgy use of (21).

If we explore the full perspective of β and long range of R (always low z), we see that intermediate parameter anyons are inhibited. We only have the fermionic sector for very low β and they do so rather insensibly to the change in R. On the other hand, as β increases, the fermionic sector vanishes completely and we are left with almost pure bosons that can condense. This behavior is a coincident result of both (21) and (24).
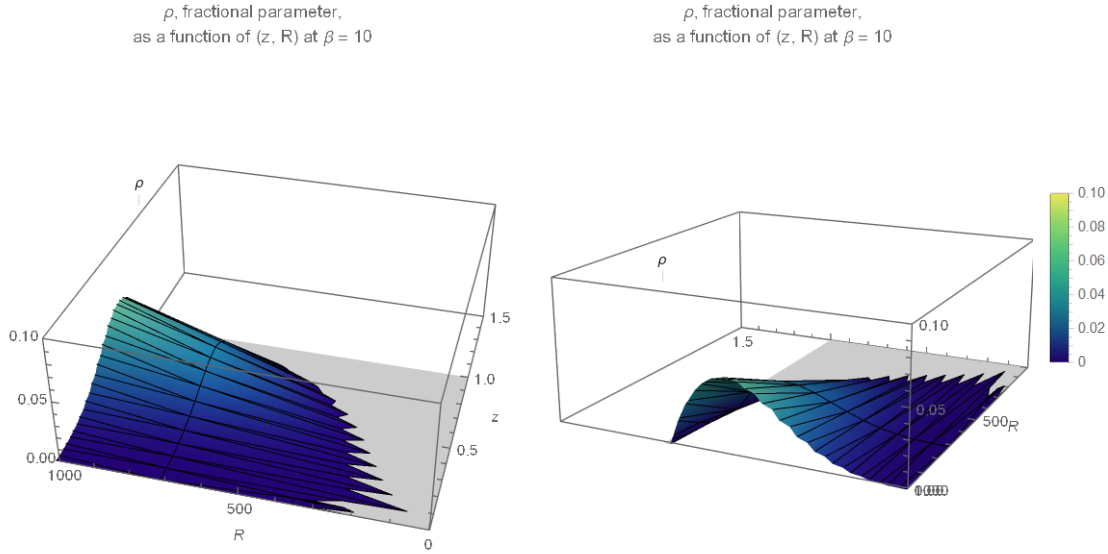

Fig 19. Fractional parameter as a function of z (in the long range) and curvature for β = 10 (3D ultrarelativistic). Fugacity was covered well beyond 1 although there are no contributions beyond that value, reason why they are not included in the captions. Carefully see that here the vertical axis (ρ value) ranges up to 0.1 only. These were obtained by numerical reversing (21) so results could only be qualitatively considered in the best of cases.
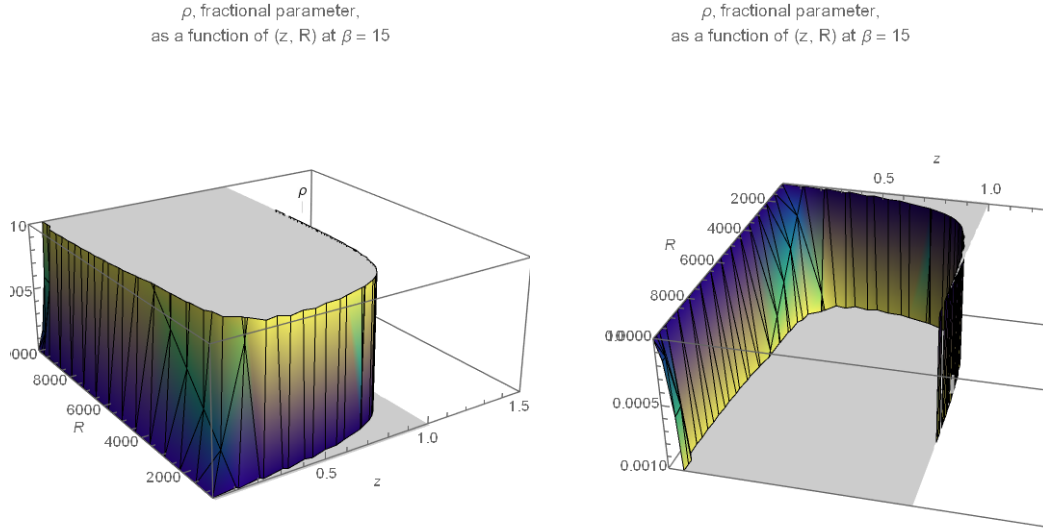
Fig 20. Fractional parameter as a function of z (in long range) and curvature for $\beta = 15$ (3D ultrarelativistic). Fugacity was covered well beyond 1 although there are no contributions past that value, reason for not including that region in the figures. See that here the vertical axis (ρ value) ranges up to 0.001 only. These were obtained by numerical reversing (21) so results could only be qualitatively considered in the best of cases.

When we move to lower temperatures, we observe the appearance of intermediate fractional parameter excitations occupying states reserved to almost pure fermionic or pure bosonic anyons at higher temperatures (c.ref. Fig. 20). This seems to take place predominantly close to flatness and for the lowest values of fugacity. Under this conditions highly bosonic anyons are almost absent in sharp contrast with almost all other values of the parameters.

4.2 Distribution of particles and internal energy for the free anyon gas from in silica approximation to $\rho(\beta, R)$.

Reversing our steps we calculate both the distribution of the number of particles and the internal energy as function of curvature by plugging (24) into (3) and (4). The results are shown in Fig. 21.
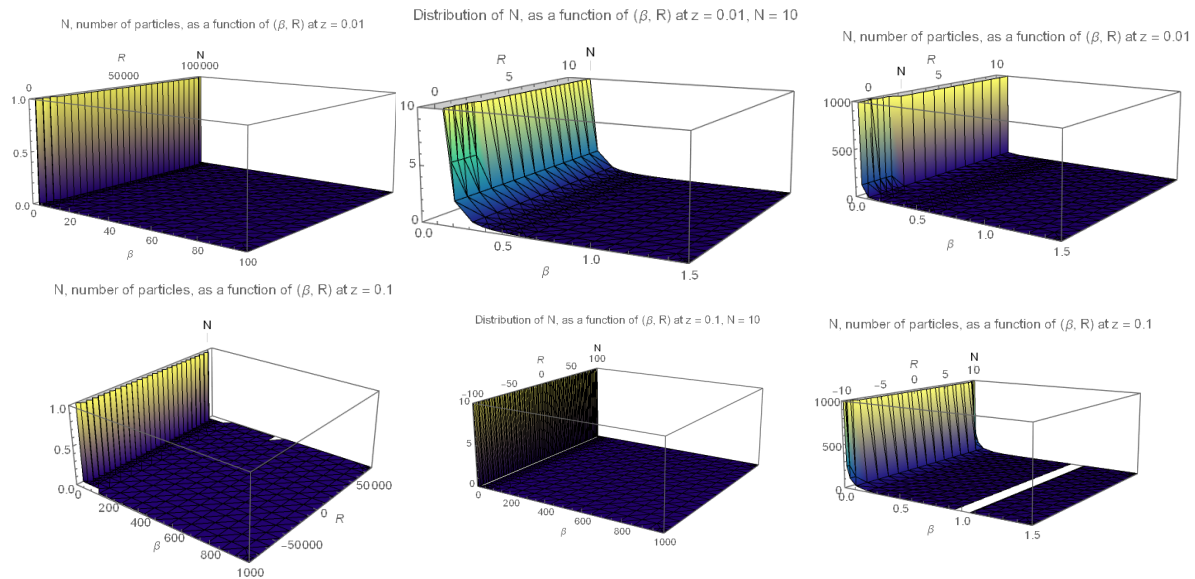

Fig.21. Distribution of the number of particles as a function of curvature and temperature at z = 0.01 for different values of N. From left to right, N = 1, N = 10, N = 1000. From (21) in the upper row, and from (24), z = 0.1, in the lower row.

Fugacity is aside in (24), so even if this seems to be a good description not only for z = 0.1, (24) works accurately only there. That said, we

observe that independently of number of particles a "Fermi surface" (in the sense described *ut supra*) develops at low β. For N = 1, where this model is not expected to be reliable at all, the interpretation could only be as a probability density for the anyon of occupying a particular fractional parameter if this could make any sense taking into account that we are dealing with an essentially statistical property, and it may just be a purely mathematical closure relation. Increasing the number of particles, and in all cases, for higher β we only have very bosonic anyons and we see that N follows the fractional parameter. For N > 1 we observe, as we did in Fig. 20, that flatness allows for intermediate values of the parameter and we learn that intermediate fractional statistics can be better observed at "the triple-low": low β, low curvature and low number of particles.

Examined at higher fugacities the behavior does not significantly differ from the exhibited at very low fugacities as can be deduced from Fig. 22 which comes from (21), which, although unreliable, matches qualitatively (24) and it does admit fugacity dependency (in fact there it is shown for a different z, 0.9 to be precise).
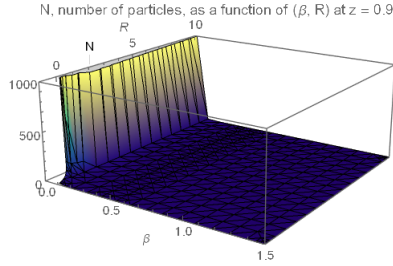

Fig. 22. Distribution of the number of particles as a function of curvature and temperature at z = 0.9 for N = 1000. Using (21).

The internal energy behaves in similar fashion although the system seems to favor storing energy from highly bosonic up to moderate fermionic anyons, not so dichotomously as the number of particles, but in a more democratic way. The non-null fermionicity sector is favoured when we are at very low β, leaving the of task to the highly bosonic partners as temperature drops (Fig. 23).
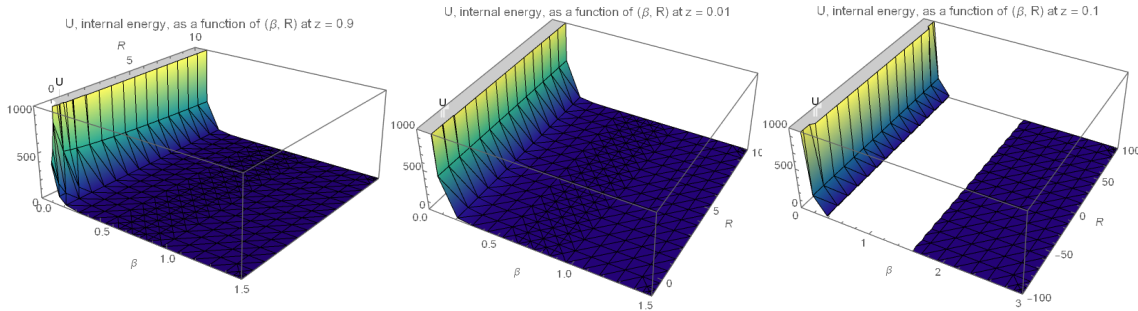

Fig. 23. The internal energy as a function of β and R for z = 0.9 and z = 0.01. Left and center, from (21). The right picture was obtained by (24).

4.3 Behavior of the fractional parameter in the vicinity of the singularity of a maximally rotating black hole

As a final application we study the distribution of the fractional parameter in the vicinity of the singularity of a maximally rotating black hole. The Ricci scalar would then as depicted in Figure 24 (actually we worked with three different values of rotation, a typical one $a \sim$ 0.6, a settled one at $a \sim 0.998$ [29] and at true $a = 1$, in the usual scale for the angular momentum: $a \in [0,1]$ is so that 0 means no rotation and 1 the maximum speed achievable, *c*)[4, 10, 11, 18]. Although it may look worthless studying the behavior of the fractional parameter so close to the singularity from an astronomer perspective, as we are deep beyond the horizon, we need to remember that in Kerr geometry, as we approach $a = 1$ the throat developed emerges a symmetry along the r parameter[10,11] allowing us to hope that results near the horizon will resemble closely those infinitesimally distant from the singularity. This motivates the ensuing use of our relation for the fractional parameter on the curvatures thereof shown in the ensuing 3D plots (Fig 24).
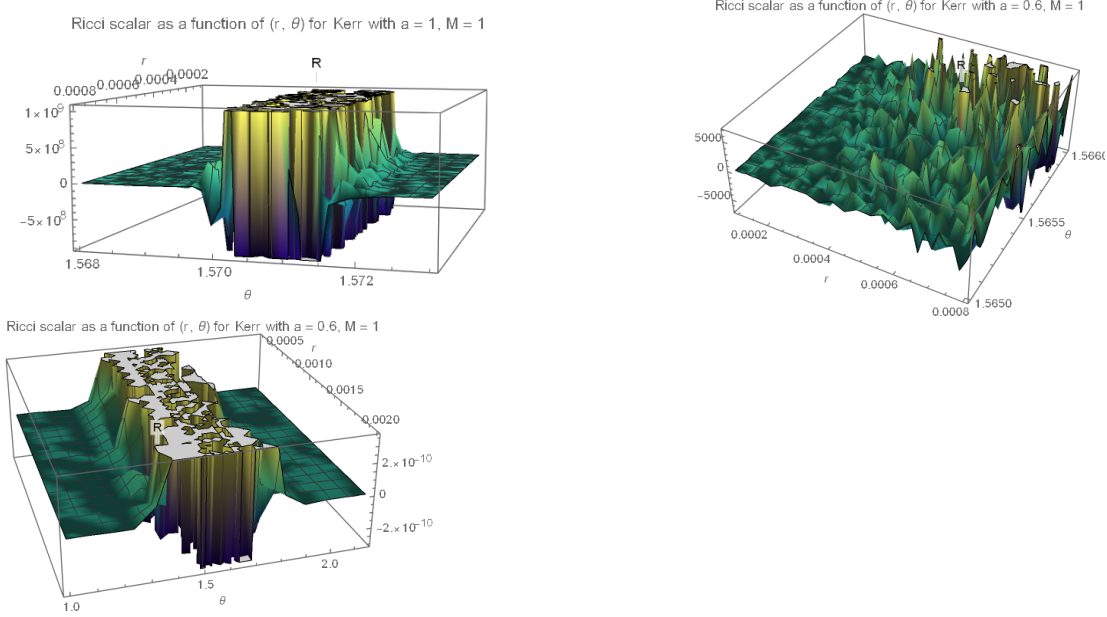
Fig. 24. Left: The curvature in the vicinity of the singularity of a Kerr black hole at maximum rotation speed. Center and right: at lower angular momentum ($a = 0.6$). These were obtained using the Black Perturbation Toolkit[30].

If we want curvature to give us the easiest result to interpret in terms of the fractional parameter, this should be the character reversal of the last one. The new branches of research in the preceding sections came from answering respective questions, in the same mood, the inquiry here reveals itself as: "is there a range of curvature for which the sectors of different fermionicity behave in opposite way to the way we observed so far?. The answer is affirmative. Immediate use of (24) give us the requested parameter values, summarized in Table 1.

Range of curvature	β	Character
$2.31983 \times 10^8 < R < 2.32216 \times 10^8$	0.1	fermionic ($0.5 < \rho < 1$)
$-2.32448 \times 10^{14} < x < 0$	100	bosonic ($0 < \rho < 0.5$)

Table 1. Conditions at $z = 0.1$ for which the fermionicity of the free ideal anyon gas appears reversed compared to the cases analyzed so far. For those values of temperature and curvature, the bosonic sector is linked to negative curvatures whereas the fermionic sector is linked to positive curvatures. This cannot be considered exhaustive as only some physically plausibly ranges were combed and (24) by itself was built up to be reliable chart at the expense of covering a smaller domain.

Under the conditions there presented, the relation between fermionicity of the sector and the curvature has flipped sign. Moreover, the ranges described by no means are exhaustive. They are obtained from (24) which is a featureless sketch of the much more complex but true (21). But even if (24) is so limited, it's not so much as not to allow these characterization reversal to bet spotted. Direct feed of the tabulated values of the first row of Table. 1 into (24) provides us with the maps for the distribution of the fractional parameter shown in Fig. 25, which on the right of the image the corresponding Ricci scalar map also plotted.
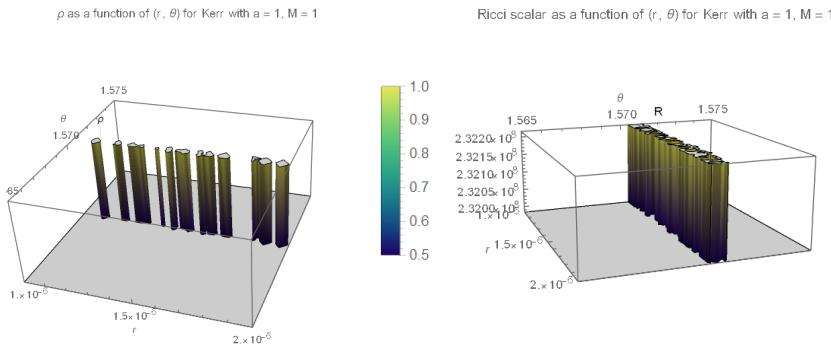

Fig. 25. Left: fractional parameter in the vicinity of the singularity of a maximally rotating Kerr black hole. For $z = 0.1$ and $\beta = 0.1$. Contrary to what was observed in the foregoing, under these conditions, the fractional parameter presents a reversed curvature-dependency

bringing the fermionic sector to positive curvatures. Right: values for the Ricci scalar over the sampled region in the left of the figure.

If instead, the values of the second row of Table 1. are used we get the results shown in Figure 26. Where for plotting purposes only the first negative slice of curvature was used $R \in [0, -1]$ (right part of the figure). In this case the bosonic sector is observed in this hyperbolic geometry.
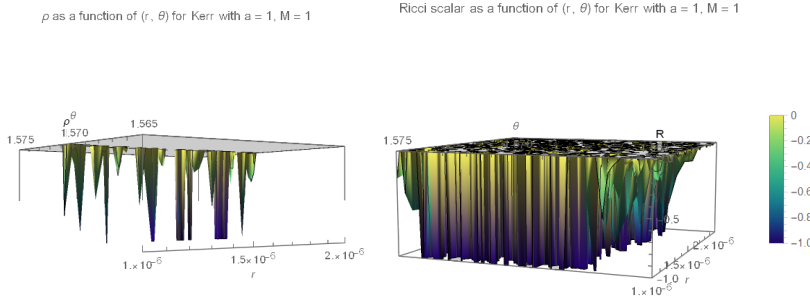

Figure 26. Fractional parameter in the vicinity of the singularity of a maximally rotating Kerr black hole. For fugacity $z = 01$. and low temperature ($\beta = 100$). Contrary to what was observed in the cases studied in the previous section, under these conditions, the fractional parameter presents a reversed curvature-dependency bringing the bosonic sector to negative curvatures. Right: values for the Ricci scalar over the sampled region in the left of the figure.

This is also observed for lowered spinning regimes, such as at the almost maximal settled rotational speed ($a = 0.998$) for which the figures are left in the notebook, and for intermediate, typical speed ($a = 0.6$), as shown in Figure 27.

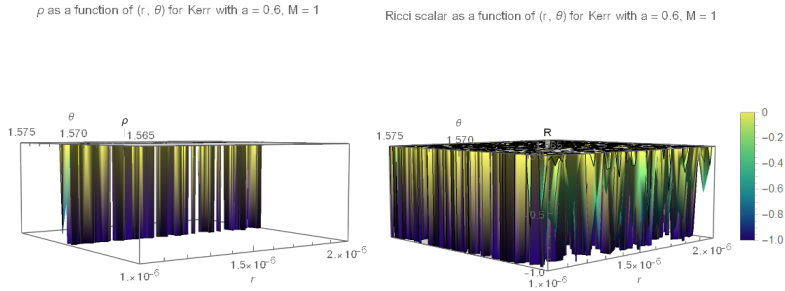Fig. 27. Figure 26. Fractional parameter in the vicinity of the singularity of a typically observed rotating Kerr black hole at slightly above half the maximal rotational speed ($a = 0.6$). For fugacity $z = 0.1$ and low temperature ($\beta = 100$). Contrary to what was observed in the foregoing, under these conditions, the fractional parameter presents a reversed curvature-dependency bringing the bosonic sector to negative curvatures and the fermionic sector to positive ones (for this last see notebook). Right: values for the Ricci scalar over the sampled region in the left of the figure.

We have gathered enough information to make a stop and see what we learned. This will be done in the following.

5. Discussion

We have come a long way, this part calls for brevity.

In the first part we built the structure to analyze the curvature of fractional statistics using the realization of it due to Polychronakos complementing the previous work by Mirza and Mohammadzadeh[16] and confirming all their results and interpretation and providing also the metric, the scalar curvature matrix and the Helmholtz free energy for the case they studied but for which they did not explicitly give the aforementioned *formulae*. We also clarified some points of their work. The plausible Cafaro-Pessoa[26] correction to the bosonic groundstate was brought to the case of generalized exclusion statistics, proving it useless away of the pure Bose-Einstein case and arguing solidly why this is so and why the possibility of physically justifying the existence of such restriction for fractional statistics seems

unsurmountable. Altogether we praise those two excellent reference works that nailed the way for us to achieve a broader and deeper understanding of the similarities and disagreements between the Physics at the surface of the fractional parameter manifold, i.e. the Bose-Einstein and Fermi-Dirac cases, and in its bulk. Summarized in a few words: Law 1 of curvature-statistics: high-parameter hyperbolic-fermionic, low-parameter spheric-bosonic. This, to be understood up to a sign convention, which makes the sign somewhat irrelevant unless under the presence of "buckling" (for what we mean, the transition of character from bosonic to fermionic for a given curvature, something that cannot be hidden under the rug of a convention if takes place).

In the second part, we allowed ourselves to explore the consequences of taking literally the maps obtained for the fractional parameter in terms of curvature, in a certain sense like relating worldsheet with target space. We inverted the map which gives curvature in terms of fractional parameter, β and fugacity and found how intricate this task, at first sight elementary, really proved to be. The payoff worth it. It allowed us to observe how the fractional parameter and derived distribution of the number of particles and internal energy would behave for different values of curvature. And furthermore, we observed that all those results can turn exactly upside down under the convulse spacetime near extreme Kerr geometry and even for intermediate rotation regimes. The equivalent summarizing aphorism here crystalizes in a way reminiscent of Thorne's mnemonic[31]: Law 2 of curvature-statistics: under certain curvatures, flip a sign.

Before we leave, we would also like to comment what we have omitted. We have not considered what could be called *überfermions* or *überbosons*, that is we assumed the fractional parameter interpolates only and not extrapolates fermions and bosons. That's the reason behind the cutoffs in the 3D plots, for example. Actually the mathematics involved allows for fractional parameters to the left of 0 and beyond 1 along the real line. The fact that the fractional parameter and the number of particles for anyons are sensible to the underlying topology as to suffer severe restrictions on their values[8, last chapter], just as we have seen here and also expressed through the internal energy, could serve as a way to probe this last by means of experimentally studying their condensation. This calls for experimental setup designs which have not been subject of any try to devise here. Finally, we neglected too the nourishment of a reliable piecewise function of ρ (β, z, R) arranged to cover the full map of values. Being the relation of curvature-statistics a topic of major concern[29] in Physics in longstanding undergoing research we are sure this will be done elsewhere.

Acknowledgments

References

[1] E. Sudarshan, I. Duck., "Pauli And The Spin-Statistics Theorem", 1998, DOI:10.1142/9789812817037

[2] Frank Wilczek, "Quanta of the Third Kind: Anyons", 2021 CAP Herzberg Memorial Public Lecture, 2021

[3] Ady Stern, arXiv:0711.4697, "Anyons and the quantum Hall effect - a pedagogical review"

[4] Robert Wald, "Quantum Field Theory on Curved Space-Times and Black Hole Thermodynamics", 1994, Chicago Press

[5] John A. Wheeler, "A Journey into Gravity and Spacetime", W H Freeman & Co (Scientific American Library), 1990

[6] Jacob D. Bekenstein, "Black Holes and Entropy", Phys. Rev. D 7, 2333 (1973)

[7] Javier Rodríguez-Laguna et al 2017 J. Phys. A: Math. Theor. 50 164001, DOI 10.1088/1751-8121/aa6268

[8] Avinash Khare, "Fractional Statistics and Quantum Theory: Second Edition", 2005, World Scientific, doi.org/10.1142/5752

[9] https://www.zdnet.com/article/microsoft-just-upped-its-multi-million-bet-on-quantum-computing/

[10]   Daniel Kapec, Alexandru Lupsasca, "Particle motion near high-spin black holes", Class. Quantum Grav. 37, 015006 (2020)

[11] Alexandru Lupsasca, Phd. Thesis Dissertation, 2017, http://nrs.harvard.edu/urn-3:HUL.InstRepos:40046542

[12] Samuel E. Gralla, Alexandru Lupsasca, Andrew Strominger, Phys. Rev. D 93, 104041 (2016), arXiv:1602.01833 [hep-th]

[13] F. D. M. Haldane, ''Fractional statistics in arbitrary dimensions: A generalization of the Pauli principle", 1991, Phys. Rev. Lett. 67, 937

[14] Frank Wilczek, Chetan Nayak, "Exclusion Statistics: Low-Temperature Properties, Fluctuations, Duality, Applications", PUPT 1466, IASSNS 94/25, arXiv:cond-mat/9405017

[15] A.P. Polychronakos, "Solitons and fractional statistics", 1996, Phys. Lett. B 365, 202, arXiv:cond-mat/9509163

[16] Behrouz Mirza, Hosein Mohammadzadeh, "Thermodynamic geometry of fractional statistics", 2010, Physical Review E 82(3 Pt 1):031137, DOI:10.1103/PhysRevE.82.031137

[17] R.P. Feynman, "Statistical mechanics: a set of lectures", Reading, Mass., W. A. Benjamin. Chicago / Turabian, (1972)

[18] Thorne, Kip S.; Blandford, Roger, "Modern Classical Physics", Princeton University Press, (2017)

[19] Yong-Shi Wu, "Statistical Distribution for Generalized Ideal Gas of Fractional-Statistics Particles", Phys. Rev. Lett. 73, 922, (1994)

[20] T. Aoyama, "Specific heat of the ideal gas obeying the generalized exclusion statistics", Eur. Phys. J. B 20, 123-131 (2001)

[21] Daniel Kapec and Alexandru Lupsasca, "Particle motion near high-spin black holes", arXiv:1905.11406v2 (2019)

[22] SN Santalla, G Ramírez, SS Roy, G Sierra, J Rodríguez-Laguna, "Entanglement links and the quasiparticle picture", 2022, Physical Review B 107 (12), L121114

[23] S. Amari, "Information Geometry and Its Applications; Applied Mathematical Sciences", Springer, 2016

[24] I. Bengtsson, K. Zyczkowski, "Geometry of Quantum States: An Introduction to Quantum Entanglement", 2nd Edition, DOI:10.1017/CBO9780511535048, (2017)

[25] H. Janyszek "Riemannian geometry and stability of thermodynamical equilibrium systems"J. Phys. A: Math. Gen. 23 477, (1990)

[26] P. Pessoa, C. Cafaro, "Information geometry for Fermi-Dirac and Bose-Einstein quantum statistics", Physica A 576, 126061 (2021)

[27] R. P. Feynman, -Morinigo, F. B. and Wagner, W. G. and Hatfield, B.- ed., "Feynman lectures on gravitation", Westview Press, (1996)

[28] Thorne, Kip S. ; Price, Richard H. ; MacDonald, Douglas A., "Black holes: the membrane paradigm", New Haven: Yale University Press, (1986)

[29] V Aldaya, M Calixto, "On a curvature-statistics theorem", J. Phys.: Conf. Ser. 128 012051 (2008)

[30] Black Hole Perturbation Toolkit, (bhptoolkit.org).

[31] "For the time component, flip a sign".

Appendix. Links to the notebooks

Many of the computations in this work where done in Mathematica® and the notebooks are provided here:

...